Journal of Sound and Vibration (2002) **257**(1), 119–130
doi:10.1006/jsvi.5034, available online at http://www.idealibrary.com on IDEAL®

A NEW METHOD FOR SEPARATING LONGITUDINAL WAVES IN A LARGE DIAMETER HOPKINSON BAR

P. J. Zhao and T. S. Lok

School of Civil and Structural Engineering, College of Engineering, Nanyang Technological University, Blk N1, Nanyang Avenue, Singapore 639798, *Singapore. E-mail: ctslok@ntu.edu.sg*

(*Received* 23 *August* 2001; *and in final form* 31 *January* 2002)

This paper outlines various methods for separating fundamental longitudinal waves propagating along a Hopkinson pressure bar. Advantages and disadvantages of the different methods are presented and discussed in detail. A new method is then proposed for separating the fundamental waves in the frequency domain. This new method is based on the assumption that wave propagation can be adequately described by the first mode of the *Pochhammer–Chree* theory. The method requires two-point strain gauge measurements on the pressure bar. Fourier components of the positive wave at one gauge location are determined either from the corresponding Fourier components of the measured strain histories or from their derivatives. The method also makes use of the derivative of the wave number with respect to the circular frequency of the pressure bar. Important points of the implementation of the technique are described. Numerical accuracy of the proposed method is verified by considering a simple example with analytical solution and by comparing measured data derived from a large diameter Hopkinson pressure bar. The proposed method will find application in dynamic material tests using the split Hopkinson pressure bar technique.

1. INTRODUCTION AND BACKGROUND TO WAVE SEPARATION

The purpose of wave separation is to determine the fundamental elastic wave propagating in two single directions of an elastic bar. These waves are obtained by measurement at one or more locations along the bar. Wave separation is useful in processing experimental data generated in long duration tests using the split Hopkinson pressure bar (SHPB) technique. Under these conditions, waves propagating in different directions are intermingled in the pressure bars whose lengths may be shorter than normally encountered in conventional practice.

Wave separation methods are classified into two broad groups: two-point and one-point measurement methods. A two-point measurement method suggested by Lundberg and Henchoz [1] assumes that strain pulses propagate in one-dimensional manner so that the strain value at one location is determined from that at another upstream location. Figure 1 illustrates a pressure bar with two strain gauges at A and B, and the wave propagation diagram. Location A is the origin of the spatial co-ordinate z and is closer to the impact end of the bar. The incident strain at location A is equal to the total strain for time $t < T$, T being the time when the reflected wave reaches location A. The incident strain at point A at time $t > T$ is determined by appropriate time-shift procedure:

$$\varepsilon_A^I(t) = \varepsilon_A(t) - [\varepsilon_B(t - \Delta t) - \varepsilon_A^I(t - 2\Delta t)], \tag{1}$$

0022-460X/02/$35.00

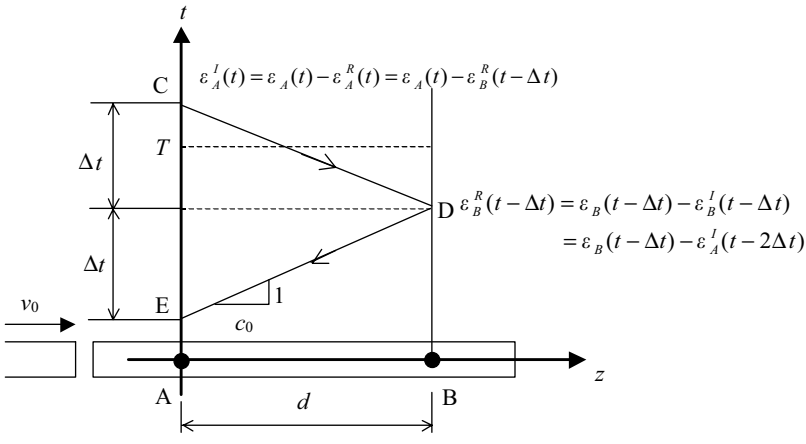

Figure 1. Strain gauge location and wave propagation diagram.

where ε_A^I is the incident strain at location A, ε_A and ε_B are the recorded total strains at locations A and B, respectively, and Δt is the time for the elastic wave to propagate from A to B. Repetitive application of equation (1) leads to the determination of ε_A^I, whose time duration is unlimited.

For the technique to be applicable to a large diameter SHPB system, the direct time shift along lines CD and DE may be substituted with a dispersion correction procedure [2], based on the *Pochhammer–Chree* dispersion equation [3, 4]. But the dispersion correction procedure requires that the first incident wave has completed itself before the reflected wave reaches location A. This leaves an undisturbed duration on the incident wave, so the specimen is loaded by a stress path with several loading/unloading cycles.

Bacon [5] proposed a new two-point method by determining the Fourier components of the positive wave at location A, $\bar{P}(\omega)$, through

$$\bar{P}(\omega) = \frac{\bar{\varepsilon}_A(\omega) - \bar{\varepsilon}_B(\omega)\exp[-k(\omega)d]}{1 - \exp[-2k(\omega)d]}, \tag{2}$$

where $\bar{\varepsilon}_A(\omega)$ and $\bar{\varepsilon}_B(\omega)$ are the spectra of strain histories recorded at locations A and B, respectively, $k(\omega)$ is the complex wave number corresponding to a given circular frequency and d is the distance between A and B. The quantity $\bar{P}(\omega)$ needs to be treated by a special iteration procedure when the denominator of equation (2) is zero. This method can be used for initial incident waves of any duration. The main disadvantage, however, is that the algorithm has to perform a lengthy iteration process.

A separation method using one-point strain measurement was proposed by Park and Zhou [6]. Essentially, this method uses the free end condition of the pressure bar as an additional natural strain measurement. However, the method extends the duration of the initial incident wave only to twice as long as classical data processing method.

2. PROPOSED WAVE SEPARATION PROCEDURE

Consider equation (2), which is derived from a general situation and where three-dimensional and viscoelastic effects are included as long as the complex wave number $k(\omega)$ is determined from an appropriate frequency equation. It is assumed that the parameter

$k(\omega)$ takes the first-mode root of the frequency equation. In developing an alternative wave separation method, equation (2) is taken as the starting point and only geometrical dispersion is considered. Thus, the complex wave number $k(\omega)$ in equation (2) is reduced to a pure imaginary number $ik(\omega)$ and equation (2) can be rewritten as

$$\bar{P}(\omega) = \frac{\bar{\varepsilon}_A(\omega) - \bar{\varepsilon}_B(\omega)\exp[-ik(\omega)d]}{1 - \exp[-i2k(\omega)d]}, \tag{3}$$

where i is the imaginary unit and $k(\omega)$ is the wave number related to frequency through

$$k(\omega) = \frac{\omega}{c(\omega)} \tag{4}$$

and in which $c(\omega)$ is the phase velocity at circular frequency ω.

Equation (3) determines $\bar{P}(\omega)$ uniquely, except at some isolated frequencies given by

$$\omega_n = n\frac{\pi c(\omega_n)}{d}, \quad n = 0, 1, 2, \ldots . \tag{5}$$

At these frequencies, $\bar{P}(\omega)$ in equation (3) is undefined. However, $\bar{P}(\omega)$ is continuous if the Fourier transform of the absolute value of the time function $|P(t)|$ exists. This is normally the case of strain signals acquired in split Hopkinson pressure bar tests. Thus, $\bar{P}(\omega_n)$ can be determined by examining the trend of $\bar{P}(\omega)$ in a neighbourhood $(\omega_n - \delta, \omega_n + \delta)$, where δ is a real number. In fact, $\bar{P}(\omega_n)$ can be replaced by its limit $\lim_{\omega \to \omega_n} \bar{P}(\omega)$.

The foregoing discussion leads to the idea that $\bar{P}(\omega_n)$ can be determined by taking the limit of the right-hand side of equation (3) as $\omega \to \omega_n$, if it exists. To confirm the existence of the limit, the numerator of equation (3) at circular frequency ω_n is calculated. The relationships between the Fourier spectra at locations A and B for single-directional waves can be found through frequency-domain solution of the wave equation, and the summation of the spectra of the single-directional waves is equal to the spectra of measured strain histories. This leads to the following relationships

$$\bar{\varepsilon}_A = \bar{P}(\omega) + \bar{N}(\omega), \tag{6}$$

$$\bar{\varepsilon}_B(\omega) = \bar{P}(\omega)\exp(-ikd) + \bar{N}(\omega)\exp(ikd), \tag{7}$$

where $\bar{P}(\omega)$ and $\bar{N}(\omega)$ are the spectra of the positive and negative waves at location A.

Eliminating $\bar{N}(\omega)$ in equations (6) and (7) and rearranging gives

$$\bar{P}(\omega)[1 - \exp(-i2kd)] = \bar{\varepsilon}_A - \bar{\varepsilon}_B\exp(-ikd), \tag{8}$$

The right-hand side must be zero at circular frequencies ω_n because the second item of the left-hand side is zero at these frequencies and $\bar{P}(\omega_n)$ is finite. Therefore, $\bar{P}(\omega_n)$ is an undefined fraction of type 0/0, and its limit can be obtained by applying L'Hôpital's rule, resulting in the expression:

$$\bar{P}(\omega_n) = \frac{\bar{\varepsilon}'_A(\omega_n) - (-1)^n\bar{\varepsilon}'_B(\omega_n) + i(-1)^n k'(\omega_n)d\bar{\varepsilon}_B(\omega_n)}{i2k'(\omega_n)d}. \tag{9}$$

Note that the right-hand side of equation (9) is fully defined and so the spectrum of the positive wave-induced strain can be determined using either equation (3) or (9). We shall call

this method, which incorporates the limit of equation (3) at singular frequencies, the *Limit Replacement Method*.

3. IMPLEMENTATION OF THE LIMIT REPLACEMENT METHOD

Equations (3) and (9) apply to the situations where wave dispersion effect caused by three-dimensional motion is considered. They are exact to the extent of the assumption that wave propagation is governed by the first mode of the *Pochhammer–Chree* theory. Earlier researchers [7–9] have demonstrated the adequacy of this assumption in tests using a conventional split Hopkinson pressure bar. Therefore, the accuracy of the wave separation method depends on its numerical implementation.

3.1. DISCRETIZATION OF THE LIMIT REPLACEMENT METHOD

An appropriate discretization scheme is adopted to implement the proposed method. Continuous Fourier transform is replaced by discrete Fourier transform (DFT) defined by

$$C_n = C(\omega_n) = \Delta t \sum_{m=0}^{N-1} F_m \exp\left(-\frac{\mathrm{i}2\pi nm}{N} \right), \tag{10}$$

$$F_m = F(t_m) = \frac{1}{T} \sum_{n=0}^{N-1} C_n \exp\left(\frac{\mathrm{i}2\pi nm}{N} \right), \tag{11}$$

where C_n is the spectrum of the nth Fourier component, F_m the signal value of the mth point of the discrete time series, Δt the sampling period, N the total number of samples and T the total duration of the time-series signal. The scaling coefficients Δt and $(1/T)$ make equations (10) and (11) approximate the continuous Fourier transform. Further, the time t_m and circular frequency ω_n are calculated as

$$t_m = m\,\Delta t, \qquad \omega_n = \frac{2\pi n}{T} = \frac{2\pi n}{N\,\Delta t}, \quad n, m = 0, 1, 2, \ldots, N-1. \tag{12}$$

The highest frequency that the discrete Fourier transform can represent is governed by the *Nyquist* frequency, which is written as

$$f_{max} = f_{N/2} = \frac{1}{2\Delta t}. \tag{13}$$

The discrete Fourier transform can be implemented by fast Fourier transform (FFT) algorithm [10]. The simplest form of FFT is obtained for a time series of $N = 2^L$ points, where L is a positive integer. To demonstrate the capability of DFT to approximate the continuous Fourier transform, consider the following non-periodic function

$$F(t) = \begin{cases} 0, & t < a, \\ \dfrac{(t-a)h}{b-a}, & a < t < b, \\ \dfrac{(c-t)h}{c-b}, & b < t < c, \\ 0, & t > c. \end{cases} \tag{14}$$

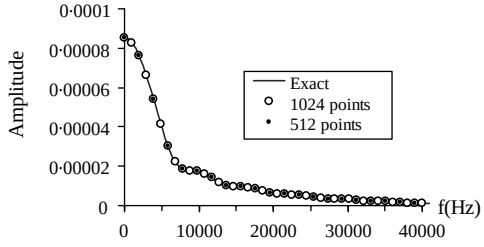

Figure 2. Amplitude spectrum of a triangular function ($a = 100\,\mu s$, $b = 120\,\mu s$, $c = 270\,\mu s$ and $h = 1$).

The amplitude of the analytical spectrum of the above triangular function ($a = 100\,\mu s$, $b = 120\,\mu s$, $c = 270\,\mu s$ and $h = 1$) is plotted in Figure 2 as a continuous line. Plotted in the same figure are the DFT amplitude spectrum ($\Delta t = 1\,\mu s$) computed through an FFT using two different signal lengths. It is observed that both DFT spectra approximate the continuous spectrum to a high degree of precision. Adding zeros to the end of the signal (e.g., 1024 points series) produces a more densely distributed spectrum.

3.2. COMPUTATION OF SPECTRAL DERIVATIVE OF STRAIN SIGNALS

Before the proposed method can be utilized, the efficiency and accuracy of the calculation of the derivative of the spectrum of a sampled signal have to be assessed because it forms part of equation (9).

The FFT gives excellent approximation for the spectrum of a discrete signal but it does not necessarily provide good results for its derivative if it is calculated by simply taking the difference of the discrete spectrum. The reason is that the frequency resolution of the FFT spectrum depends on the total duration of the signal. The sampling period cannot be larger than a certain limit for the spectrum to represent the highest harmonic component. It follows that the number of points in the time series must be as large as possible in order to obtain a satisfactory result of the spectrum derivative. This requirement is necessary because the spectrum changes rapidly at some frequency range.

Consider the triangular function of equation (14). The real part of the spectral derivative calculated by analytical and by two-point forward difference is plotted in Figure 3. Although 1024-point FFT provides a very good approximation of the spectrum, the plot indicates otherwise with respect to the spectral derivative. The result of 4096-point FFT (by adding zeros) improves the accuracy significantly but it may still be regarded as inaccurate in the low-frequency range. To overcome this difficulty, a different method has been devised.

For a transient signal whose value is non-zero in a limited time range, the continuous Fourier transform is defined as

$$C(\omega) = \int_0^T F(t) e^{-i\omega t}\, dt, \tag{15}$$

where T is the time duration comprising non-zero range of the time function $F(t)$.

Taking the derivative of $C(\omega)$ with respect to ω leads to

$$\frac{dC(\omega)}{d\omega} = -i \int_0^T t F(t) e^{-i\omega t}\, dt. \tag{16}$$

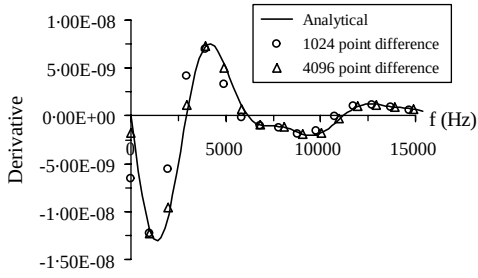

Figure 3. Comparison of the real part of spectral derivative.

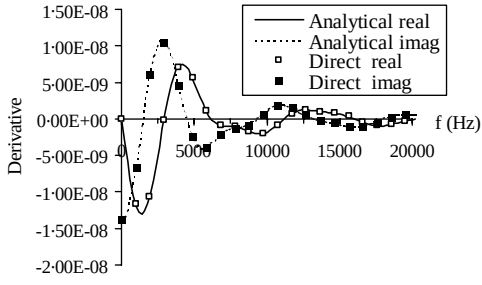

Figure 4. Spectral derivative by analytical and direct methods.

This expression relates the derivative of the spectrum to the spectrum of a new function $tF(t)$. Hence, the spectral derivative of a sampled signal $\{F(i\Delta t), i = 0, 1, 2, \ldots, N-1\}$ can be determined to high accuracy by applying FFT to the series $\{i\Delta t\ F(i\Delta t),\ i = 0,\ 1,\ 2, \ldots, N-1\}$. We shall refer to this as the Direct Method.

Figure 4 shows a comparison of the real and imaginary parts of the spectral derivative of the triangular function with analytical solution. A total of 1024 points was used for the Direct Method calculation. The result is in excellent agreement with the exact solution for the entire frequency range (including zero frequency).

3.3. DETERMINATION OF THE DERIVATIVE OF WAVE NUMBER $k'(\omega)$

The *Pochhammer–Chree* frequency equation relates many parameters, and may be described by

$$\frac{2\alpha}{a}(\beta^2 + k^2)\mathrm{J}_1(\alpha a)\mathrm{J}_1(\beta a) - (\beta^2 - k^2)^2\mathrm{J}_0(\alpha a)\mathrm{J}_1(\beta a) - 4k^2\alpha\beta\mathrm{J}_1(\alpha a)\mathrm{J}_0(\beta a) = 0, \qquad (17)$$

where a is the radius of the bar, J_0 and J_1 are 0th and 1st order Bessel's functions of the first kind, k is the wave number, and α and β are parameters related to the circular frequency ω and wave number given by

$$\alpha = \sqrt{\frac{\omega^2}{c_1^2} - k^2}, \qquad \beta = \sqrt{\frac{\omega^2}{c_2^2} - k^2} \qquad (18)$$

and in which c_1 and c_2 are dilatational wave velocity and shear wave velocity respectively. Parameters a, c_1 and c_2 are known constants for a given pressure bar.

Substituting equation (18) into equation (17) leads to a complicated non-linear equation relating two variables: k and ω. Solving this equation gives the wave number k as a function of ω. It can be shown that there are an infinite number of roots to equation (17) for a single ω. Only the first root is sought in this research because of the first-mode assumption.

Equation (17) can also be written in terms of dimensionless variables as [11]

$$f(x, \beta_v, ka) = (x-1)^2 \varphi(ka\sqrt{\beta_v x - 1}) - (\beta_v x - 1)[x - \varphi(ka\sqrt{2x-1})] = 0, \qquad (19)$$

where

$$\beta_v = \frac{1-2v}{1-v}, \qquad \varphi(y) = \frac{y\mathrm{J}_0(y)}{\mathrm{J}_1(y)}, \qquad x = (1+v)\left(\frac{c}{c_0}\right)^2, \qquad ka = \pi\frac{D}{L} \qquad (20\text{–}23)$$

in which k is the wave number, v the Poisson ratio, c the phase velocity, c_0 the bar vpelocity, D the bar diameter and L the wavelength.

The first-mode solution can be expressed by the following relationship for a given v:

$$\frac{c}{c_0} = g\left(\frac{D}{L};\, v\right), \qquad (24)$$

where c/c_0 and D/L are ratios of phase velocity to bar velocity and bar diameter to wave length respectively.

Numerical solution of equation (19) was derived by Bancroft [11] but the resolution is inadequate for calculating the derivative of the wave number. In another attempt, Davies [7] solved the frequency equation, obtaining numerical results that are in good agreement with Bancroft's data. However, Davies did not provide the necessary data of his results.

In the present investigation, equation (19) is solved numerically to derive a high-precision derivative of wave number. Modified Bessel's functions are substituted for Bessel's functions with a pure imaginary argument and approximate expressions for small arguments are used. A comparison with Bancroft's data [11] shows that our numerical solution is identical up to the fifth digit after the decimal point. Once the relationship between c/c_0 and D/L is established, the derivative of the wave number can be calculated from

$$k'(\omega) = \frac{1}{c_0 h(\omega)}, \qquad (25)$$

$$h(\omega) = \frac{c}{c_0} + \frac{D}{L}\frac{d(c/c_0)}{d(D/L)}. \qquad (26)$$

It is noted that $k'(\omega)$ of a *Pochhammer–Chree* bar is similar to that of a one-dimensional bar but with a modification factor $h(\omega)$. Both the relationship between c/c_0 and D/L and that between $h(\omega)$ and D/L are shown in Figure 5 for $v = 0{\cdot}3$.

3.4. WAVE SEPARATING PROCEDURE

According to basic wave theory, the dimensionless wave number and dimensionless frequency at each D/L can be calculated from the solution of frequency equation as

$$\bar{f} = \frac{f}{c_0/D} = \frac{c}{c_0}\frac{D}{L}, \qquad (27)$$

$$\bar{k} = \frac{k}{2\pi/D} = \frac{D}{L}. \qquad (28)$$

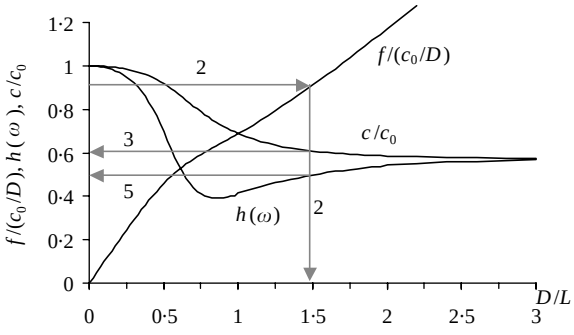

Figure 5. Characteristics of *Pochhammer–Chree* equation (numbers correspond to the steps in the separation procedure).

Three relations can then be developed and these are inter-related to determine (1) D/L from known $\bar{f}$, (2) c/c_0 from D/L and (3) $h(\omega)$ from D/L. These relations are plotted in Figure 5 for $\nu = 0{\cdot}3$.

To separate the waves, the following steps should be completed successively:

(1) Spectral analysis is performed through FFT to obtain the spectra and derivative of the spectra of the recorded strain–time histories at locations A and B.
(2) Calculate $\bar{f}$ using the first part of equation (27) for each Fourier component of frequency f_i ($i = 0, 1, 2, \ldots, N-1$). Determine D/L corresponding to $\bar{f}$ by interpolation.
(3) Calculate wave number using equation (28) from known D/L. Determine c/c_0 by interpolation from the known D/L. Calculate the phase velocity from c/c_0.
(4) The condition of equation (5) is checked.
(5) Determine $\bar{P}(\omega_i)$ using equation (3) if equation (5) is not satisfied. If equation (5) is satisfied for some integer m, equation (9) has to be used to determine $\bar{P}(\omega_m)$. Before doing this, $h(\omega)$ is found by interpolation from known D/L and then $k'(\omega)$ by using equation (25).
(6) After processing all frequency components, inverse FFT is used to compute $P(t)$, the time-domain function of the positive wave at location A.

3.5. EXAMPLE OF ONE-DIMENSIONAL ELASTIC WAVE

The triangular wave discussed earlier is used as an example to illustrate the capability of the proposed method. The strain is measured at locations A and B, and B is 0·75 m downstream of A. The assumed measured triangular strain histories are shown in Figure 6. According to one-dimensional wave theory, the strain history observed at location B has exactly the same shape as that at location A but it is delayed by 150 μs ($c_0 = 5000$ m/s).

Zero frequency component of function $P(t)$ was determined using the Limit Replacement Method. In addition, the 257th Fourier component has circular frequency of 1570796·3 rad/s, which is 74·99999981 times ω_0 (20943·950667). The Fourier coefficient of this component calculated by equation (3) has a real part ($8{\cdot}29 \times 10^{-4}$) and an imaginary part ($8{\cdot}2937 \times 10^{-4}$). But the more accurate coefficients are calculated as the real part ($-3{\cdot}76 \times 10^{-9}$) and the imaginary part ($1{\cdot}04 \times 10^{-8}$) by using the Limit Replacement Method—equation (9)—with $n = 75$. Clearly, the computational error caused by the small

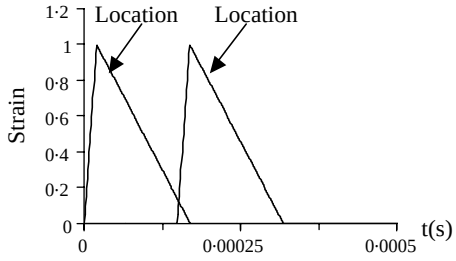

Figure 6. Measured strain histories in example problem.

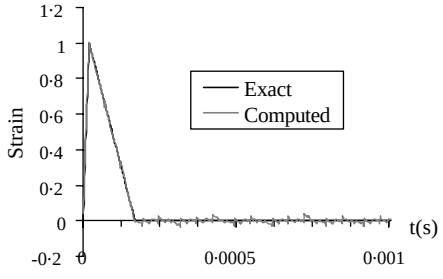

Figure 7. Computed and exact positive wave at location A.

denominator in equation (3) could approach several orders of magnitude higher than the true Fourier coefficient at some frequencies. The function $P(t)$ obtained by the analytical and the proposed method ($N = 1024$ and $\Delta t = 1\,\mu s$) is plotted in Figure 7. The results are in excellent agreement.

4. VALIDATION OF THE PROPOSED WAVE SEPARATION METHOD

To validate the proposed wave separation method, an experiment was conducted to generate the strain wave in a 75 mm diameter, 1·5 m long pressure bar ($\nu = 0{\cdot}3$ and $c_0 = 5155$ m/s) made of high strength steel [12], shown in Figure 8(a). The bar is instrumented with a single resistance strain gauge at mid-length. The strain wave is generated by the impact of a 0·54 m long solid cylindrical striker of the same diameter and same material. The strain gauge records the strain pulses induced by the first incident wave and subsequent reflected waves separately.

Reflection at the right end changes the incident wave from compressive to tensile but does not change its amplitude. So, the reflected wave recorded at the gauge location, after allowing for reversal of sign, is essentially the same as the strain wave which would be recorded at half length of the incident bar from the free end of an imaginary extension of the incident bar. The problem becomes that of separating the waves from the strain histories measured at locations A and B, which are 1·5 m apart. Similarly, the gauge distance becomes a multiple of 1·5 m if the strain history after multiple reflections is used. In this paper, the strain histories of the first incident wave and the second reflected wave are used to emphasize the dispersion effect, so the distance between locations A and B is 3 m.

It is recognized that the best way of validating a wave separation method is to process the experimental data recorded by two strain gauges. For our equipment, this is difficult

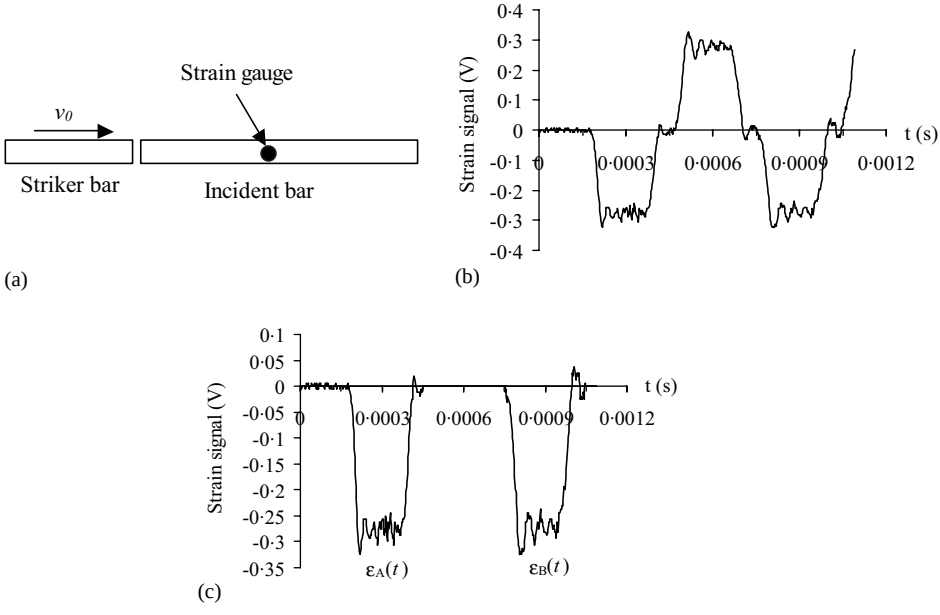

Figure 8. (a) Experimental set-up in large diameter bar example. (b) Measured strain signal in larger diameter bar example. (c) Two strain histories used in large diameter bar example.

because of the short pressure bar. The length/diameter ratio of 20 necessitates mounting the strain gauge in the middle of the bar so that the wave satisfies the *Pochhammer–Chree* theory at 10 times diameter away from the ends. But two-gauge records can be simulated by the single-gauge configuration based on the above description. In addition, this procedure has an advantage that the exact positive wave at location A is known.

The gauge record is shown in Figure 8(b). It can be observed that the shape of the second negative pulse differs from the first negative pulse. This shows the dispersion occurs after the wave travels 3 m along the pressure bar. So, dispersion correction may be necessary in separating waves. The two strain histories used in separation are illustrated in Figure 8(c), which is extracted from the curve in Figure 8(b) by cutting its first and third pulses and adding zeros before the beginning and after the end of each pulse.

The strain history of the positive wave at location A is shown in Figure 9. Three strain histories are plotted. They are: (1) the exact solution, (2) the strain history separated by the proposed method with consideration of wave dispersion, and (3) the strain history separated by the proposed method without consideration of wave dispersion.

It is observed from Figure 9 that the one-dimensional result differs considerably from the exact solution, which is especially manifested by the disagreement of the troughs and peaks in the two curves. The three-dimensional separation improves the result significantly by incorporating dispersion correction into wave separation process. The three-dimensional result matches the exact solution better in the rise-up phase.

It is well-known that high-frequency components are distorted during propagation because of dispersion. Therefore, one-dimensional separation methods, ignoring dispersion effect, can produce acceptable results only in the low-frequency range. The methods break down if the recorded wave contains significant high-frequency components. Three-dimensional wave separation method, such as the proposed method, avoids this problem. This point was also discussed in reference [5].

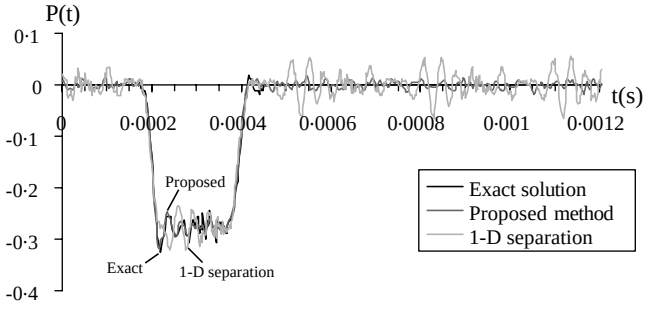

Figure 9. Result of separation of large diameter bar example.

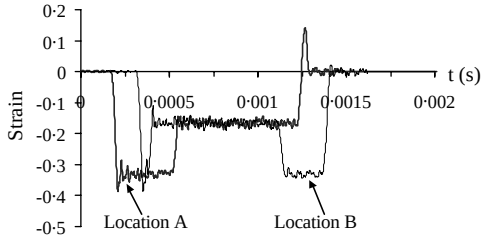

Figure 10. Strain histories at locations A and B — second example.

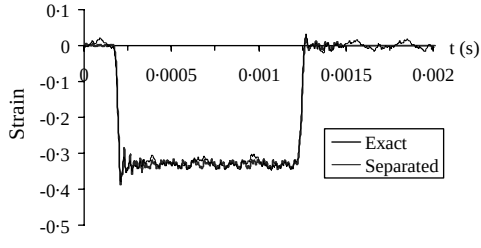

Figure 11. Result of separation of the second example.

A second example is given to demonstrate the capability of the proposed method for processing the strain records with intermingled positive and negative waves. The strain histories recorded at locations A and B (0·75 m away from each other) are shown in Figure 10 and they are constructed from the known positive and negative waves at both locations. This is a numerical example corresponding to an infinitely slender bar because dispersion is intentionally excluded in construction of the waves. This example also shows the performance of the proposed method in separating intermingled waves in a very small diameter pressure bar. In the computation, the bar diameter is taken as 1 mm to eliminate the dispersion effect.

Figure 11 shows a comparison between the exact and separated positive waves at location A. The positive wave has been reconstructed successfully from recorded total waves. This is especially demonstrated by the correct removal of the negative wave when it interferes with the positive wave. In addition, the head of the pulse is very accurate.

5. CONCLUSIONS

(1) A method has been developed and this has been used successfully to separate the fundamental waves propagating along a *Pochhammer–Chree* pressure bar.
(2) Unlike other methods, the proposed technique uses full frequency-domain separation and does not impose any limit to the time duration of the first incident wave. Implementation of the technique does not require a lengthy iteration procedure.
(3) Examples show that by incorporating dispersion correction in wave separation, the accuracy of the computed result is significantly improved.

REFERENCES

1. B. LUNDBERG and A. HENCHOZ 1977 *Experimental Mechanics* **17**, 213–218. Analysis of elastic waves from two-point strain measurement.
2. H. ZHAO and G. GARY 1997 *Journal of Mechanics and Physics of Solids* **45**, 1185–1202. A new method for the separation of waves: application to the SHPB technique for an unlimited duration of measurement.
3. L. POCHHAMMER 1876 *Journal fur die Reline und Angewandte Mathematik* **91**, 324–326. On the propagation velocities of small oscillations in an unlimited isotropic circular cylinder.
4. C. CHREE 1889 *Cambridge Philosophical Society, Transactions* **14**, 250–369. The equations of an isotropic elastic solid in polar and cylindrical coordinates, their solutions and applications.
5. C. BACON 1999 *International Journal of Impact Engineering* **22**, 55–69. Separation of waves propagating in an elastic or viscoelastic Hopkinson pressure bar with three-dimensional effects.
6. S. W. PARK and M. ZHOU 1999 *Experimental Mechanics*. **39**, 287–294. Separation of elastic waves in split Hopkinson bars using one-point strain measurements.
7. R. M. DAVIES 1948 *Philosophical Transactions A* **240**, 375–457. A critical study of the Hopkinson pressure bar.
8. P. S. FOLLANSBEE and C. FRANTZ 1983 *Journal of Engineering Materials and Technology* **105**, 61–66. Wave propagation in the split Hopkinson pressure bar.
9. J. C. GONG, L. E. MALVERN and D. A. JENKINS 1990 *Journal of Engineering Materials and Technology* **112**, 309–314. Dispersion investigation in the split Hopkinson pressure bar.
10. J. W. COOLEY and J. W. TUKEY 1965 *Mathematics of Computation* **19**, 297. An algorithm for the machine calculation of complex Fourier series.
11. D. BANCROFT 1941 *Physical Review* **59**, 588–593. The velocity of longitudinal waves in cylindrical bars.
12. T. S. LOK, X. B. LI, D. S. LIU and P. J. ZHAO *American Society of Civil Engineers Journal of Materials in Civil Engineering*. Testing and response of large diameter brittle materials subjected to high strain rate (in press).